Catal Lett (2012) 142:728–735
DOI 10.1007/s10562-012-0820-6

Steam Reforming on Transition-Metal Carbides from Density-Functional Theory

Aleksandra Vojvodic

Received: 9 September 2011 / Accepted: 31 March 2012 / Published online: 21 April 2012

Abstract A screening study of the steam reforming reaction on clean and oxygen covered early transition-metal carbides surfaces is performed by means of density-functional theory calculations. It is found that carbides provide a wide spectrum of reactivities, from too reactive via suitable to too inert. Several molybdenum-based systems are identified as possible steam reforming catalysts. The findings suggest that carbides provide a playground for reactivity tuning, comparable to the one for pure metals.

Keywords DFT · Steam reforming · Carbides · Surfaces · Reactivity trends

1 Introduction

Steam reforming is an important industrial process, where natural gas (CH_4) is converted into synthesis gas (CO and H_2) according to the overall reaction

$$CH_4 + H_2O \rightleftharpoons CO + 3H_2. \quad (1)$$

The synthesis gas is subsequently transformed into more valuable chemicals, such as ammonia, methanol, and diesel. Since steam reforming acts as a source of hydrogen, it is also potentially important for any emerging hydrogen economy. For a detailed review of the steam reforming process and its applications see for example Ref. [1].

Commercially the steam reforming reaction is conducted over a Ni-based catalyst due to the relatively low cost and good activity of nickel. This reaction has been studied in detail on the close-packed Ni(111) surface and on the stepped Ni(211) surface by means of density-functional theory (DFT) [2]. The major technological challenge for Ni catalysts is the formation of carbonaceous deposits, termed coke, that lead to catalyst deactivation. In Refs. [2, 3] it was established that the step edges on Ni surfaces act as growth centers for graphite. Other transition metals (TM), such as Ru, Rh, Pd, Ir, and Pt also show high activity and selectivity towards steam reforming [4] and have a high resistance against carbon formation. However, these materials are scarce in nature and expensive. Therefore new materials that are resistant to carbon formation are needed.

Transition-metal carbides (TMC's) have gained quite some attention since Levy and Boudart reported that they have "platinum-like behavior" for certain reactions [5]. The starting material for the production of carbides is cheap and abundant and therefore it has been suggested that they can replace the noble metals in catalysis. The main problem with the carbides has been to produce materials with sufficiently high surface area for them to be interesting for catalytic applications. This problem has been overcome and several studies report on carbides with surface areas as high as 200 m^2/g [6–9].

In Refs. [10, 11], it was shown that carbides of molybdenum and tungsten are stable and active catalysts for not only the steam reforming but also the dry reforming and the partial oxidation of methane at elevated pressures.

A. Vojvodic
Department of Applied Physics, Chalmers University of Technology, Göteborg 412 96, Sweden

A. Vojvodic (✉)
SUNCAT Center for Interface Science and Catalysis,
SLAC National Accelerator Laboratory, 2575 Sand Hill Road,
Menlo Park, CA 94025, USA
e-mail: alevoj@slac.stanford.edu

A. Vojvodic
Department of Chemical Engineering, Stanford University,
Stanford, CA 94305, USA

Moreover, no macroscopic carbon was deposition on the catalysts during the catalytic reactions. The relative activity of a number of steam reforming catalysts was established as: Ru > Rh > Ir $\approx$ Mo_2 C > WC > Pd > Pt.

Several DFT studies concerning adsorption on TMC's have been conducted, for example, atomic adsorption [12–20], O_2 adsorption [21], CO adsorption [22–24], NH_x ($x = 1 - 3$) adsorption [19, 20], methanol adsorption [25], CH_x ($x = 0 - 3$) and C_2H_4 adsorption [26]. In addition, the water–gas-shift reaction has been studied in Refs. [27–29].

To our knowledge, a theoretical understanding of the steam reforming reaction on TMC's is missing in the literature. The aim of this paper is to investigate how the TMC's are suited for the steam reforming reaction by performing a set of DFT calculations on different surfaces of α-Mo_2C, TiC, VC, and δ-MoC in order to catch the trends between TMC's composed of different TM atoms and of different structures. The influence of the surfaces being covered with oxygen is also investigated.

The outline of this paper is as follows. To begin with the systems to be investigated are defined in Sect. 2. This is followed by Sect. 3, which describes the calculation details. Our results are presented in Sect. 4 and discussed in Sect. 5. The paper ends with a conclusion in Sect. 6.

2 Investigated TMC Systems

The Mo–C system can occur in several crystalline forms, see for example the phase diagrams in Refs. [30, 31]. There are two types of Mo_2C phases, one orthorhombic (α) and one hexagonal (β), which is a high temperature phase. In this study, we focus on the α phase. For this phase the Mo atoms are only slightly distorted from an hcp arrangement and the carbon atoms occupy one half of the octahedral interstitial sites. In the present molybdenum carbide literature there seems to be a confusion when it comes to the attribution of the symbols to the different phases, especially regarding the α and β phases. This is probably because the α-Mo_2C phase was originally assigned a hexagonal structure but refined experiments identified the structure to be of orthorhombic type [32], with lattice parameters $a = 4.729$ Å, $b = 6.028$ Å and $c = 5.197$ Å [33].

The close-packed surface of α-Mo_2C is the (100) surface. It consists of alternating Mo and C layers and can be either Mo- or C-terminated. Experimental studies of α-Mo_2C(100) show that the surface termination and structure depend strongly on the cleaning procedure. Both the Mo- and the C-terminated surfaces have been observed [34, 35]. Therefore we consider both the TM- and the C-terminated carbide surfaces.

The TiC, VC and δ-MoC adopt the NaCl structure. The (100) surface of these carbides consists of layers of equal amounts of TM and C atoms. The (111) surface, however, is polar and consists of alternating TM and C layers, similar to the α-Mo_2C(100) surfaces. One important difference is that the C-terminated α-Mo_2C(100) surface has half the amount of C atoms as compared to a C-terminated TMC(111) surface.

In this paper, we report the results from DFT calculations on (i) the TM- and C-terminated surfaces of α-Mo_2C(100), TiC(111), VC(111), and δ-MoC(111); (ii) the O-covered surfaces in (i); and (iii) the (100) surfaces of TiC, VC and δ-MoC.

3 Theoretical Details

All the DFT calculations are performed with the computer code DACAPO [36], which uses plane-waves and ultra-soft pseudopotentials. For the optimization of the bulk lattice parameters of the considered TMC's a plane-wave cutoff of 400 eV, a $8 \times 8 \times 8$ k-point sampling, and the RPBE exchange-correlation functional [37] are used. The bulk structure of α-Mo_2C was obtained by minimizing the total energy of the unit cell with respect to the length of the lattice vectors using a Newton–Raphson scheme and allowing for complete internal relaxation at each step. The calculated lattice parameters $a = 4.825$ Å, $b = 6.162$ Å, and $c = 5.304$ Å differ by ~ 2 % from the experimental values [33].

For TiC, VC and δ-MoC, the equilibrium bulk structure was obtained utilizing the Murnaghan equation of state [38]. The calculated lattice constants are 4.336, 4.171, and 4.444 Å for TiC, VC, and δ-MoC, respectively. A quantitative agreement is found between the theoretical and experimental lattice constants [39, 40].

The surfaces are modeled using the supercell approach, with the DFT lattice parameters given above. A 400 eV energy cutoff for the plane-wave expansion of the one-electron orbitals, a $4 \times 4 \times 1$ k-point grid, and the RPBE functional are used. Each TMC(111) and TMC(100) surface is represented by a slab with the geometry defined in Fig. 1 and a thickness of four atomic layers. Repeated slabs are separated by at least a 10.8 Å thick vacuum region. The Mo- and C-terminated α-Mo_2C(100) slabs have a surface geometry as defined in Fig. 1 and consist of four layers Mo and four layers C separated by 10.6 Å vacuum. During structural relaxations, the two bottom atomic layers are constrained to the corresponding bulk geometry.

Figure 1 shows the relaxed structures of the Mo- and C-terminated δ-MoC(111) surfaces, the δ-MoC(100) surface, and the Mo- and C-terminated α-Mo_2C(100) surfaces. These relaxed surfaces and the corresponding VC and TiC surfaces are used as starting points for the modeling of the steam reforming reaction.

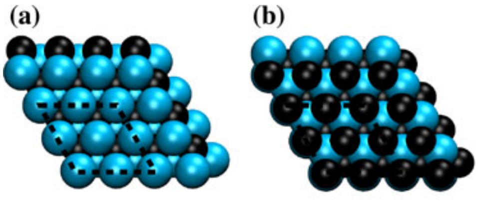

Fig. 1 Top view of the relaxed: **a** Mo-terminated δ-MoC(111), **b** C-terminated δ-MoC(111), **c** δ-MoC(100), **d** Mo-terminated α-Mo_2C(100), **e** C-terminated α-Mo_2C(100) surface. The *blue* and *black balls* represent the Mo and C atoms, respectively. The *black dashed lines* indicate the unit cell

The investigated steam reforming reaction is assumed to have the following nine elementary steps:

$$CH_4 + 2^* \rightleftharpoons CH_3^* + H^* \tag{2}$$

$$CH_3^* +^* \rightleftharpoons CH_2^* + H^* \tag{3}$$

$$CH_2^* +^* \rightleftharpoons CH^* + H^* \tag{4}$$

$$CH^* +^* \rightleftharpoons C^* + H^* \tag{5}$$

$$H_2O + 2^* \rightleftharpoons OH^* + H^* \tag{6}$$

$$OH^* +^* \rightleftharpoons O^* + H^* \tag{7}$$

$$C^* + O^* \rightleftharpoons CO^* \tag{8}$$

$$CO^* \rightleftharpoons CO +^* \tag{9}$$

$$2H^* \rightleftharpoons H_2 + 2^*, \tag{10}$$

where * (2*) denotes one (two) empty surface site and X* denotes the adsorbate X bonded to this site. This paper is based on an adsorption energy analysis. Such a thermodynamic analysis has previously been proven to be able to predict reactivity trends for metals [4]. There are two main reasons for this. First, the adsorption energy difference from one metal to the next are large. Second, there is a correlation between adsorption energies and energy barriers, the so called Brønsted–Evans–Polanyi relations, previously found on metals [41] and a group of carbides [20]. Hence, the reactivity of a material can to a first order be obtained directly from a thermodynamic analysis.

In this study we consider adsorption of all the intermediates (CH_3, CH_2, CH, C, OH, O, CO, and H) in Eqs. (2)–(10). In all adsorption calculations, the adsorbate coverage is one-quarter of a monolayer (ML) relative to the number of TM atoms in the surface (subsurface layer if the surface is C terminated). Adsorption is allowed on one of the two slab surfaces at the time. Adsorbates together with the surfaces are allowed to relax in all directions until the forces are less than 0.05 eV/Å. The energies in the calculated potential energy diagrams are expressed relative to the clean surface (O-covered surfaces if the surface is oxygenated), a CH_4 molecule, and a H_2O molecule in the gas phase.

The steam reforming reaction on the oxygenated TMC surfaces is modeled by adsorbing the reaction intermediates on a 1ML O-covered TMC surface. According to DFT calculations in Ref. [28], the O covering of the Mo- and C-terminated Mo_2C(100) surfaces is energetically favorable up to 1ML. Our calculations give the same structure for the 1ML O-covered Mo- and C-terminated Mo_2C(100) surfaces as in Ref. [28].

4 Results

This section focuses on the results obtained from the screening calculations study. We provide the calculated potential energy diagrams for the steam reforming reaction on all the considered TMC surfaces. These are compared with existing results on Ni(111) and Ni(211) [2].

4.1 TMC(111) and α-Mo_2C(100) Surfaces

The calculated potential energy diagram for the steam reforming reaction on the TM- and C-terminated TMC's is shown in Fig. 2. First of all we notice that the span of the potential energies of the investigated surfaces is huge. Compared to the Ni surfaces [2], all these TMC surfaces are much more reactive because they bind the intermediates too strongly. Therefore none of these surfaces is suitable for the steam reforming reaction.

In the following we present the trends in reactivity that are found when changing the TM atom in the TMC compound. For each of the considered TMC's, the C-terminated surface is found to be more reactive than the TM-terminated one. This is to be expected for the monocarbides since the TMC(111) surfaces are found to be TM terminated under UHV conditions [42, 43]. All the TM-terminated TMC(111) surfaces have similar potential energy shape as a function of the reaction intermediates. The same is found for the C-terminated group of TMC surfaces. For the TM-terminated TMC surfaces, the reactivity can be ordered as TiC(111) > VC(111) > α-Mo_2C(100) > δ-MoC(111), while for the C-terminated TMC surfaces we find that the reactivity order is TiC(111) > VC(111) > δ-MoC(111) > α-Mo_2C(100). Hence different trends are observed for the different terminations.

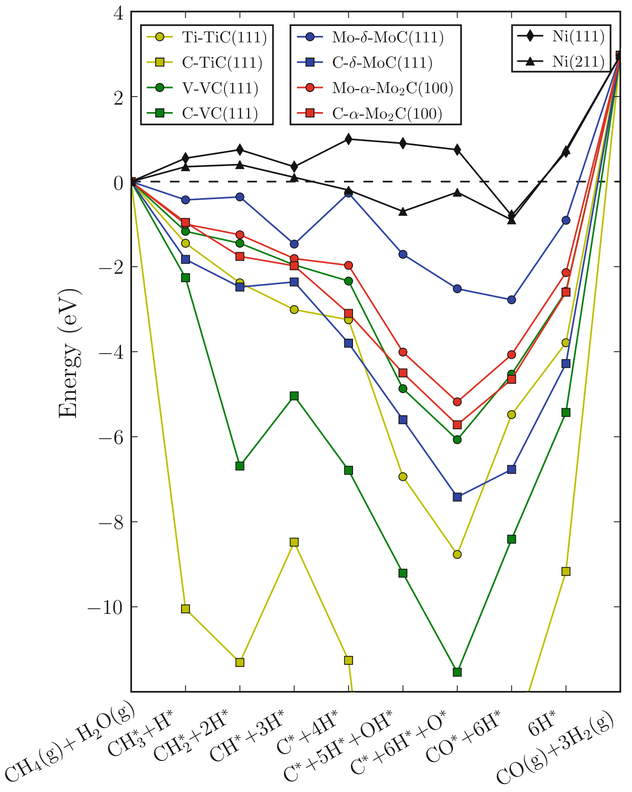

Fig. 2 Calculated potential energy diagram for the steam reforming reaction on the TM-terminated (*circles*) and C-terminated (*squares*) TMC(111) and α-Mo_2C(100) surfaces. For comparison the Ni(111) and Ni(211) data, adapted from Ref. [2], are given

The considered α-Mo_2C(100) surfaces are less reactive than the C-terminated δ-MoC(111) surface but more reactive than the Mo-terminated δ-MoC(111). For a given carbide, the smallest difference in reactivity between the TM- and the C-terminated surfaces is found for α-Mo_2C(100). This can be due to the fact that the C-terminated α-Mo_2C(100) surface has 50 % less C than the C-terminated TMC(111) surfaces.

The largest energy change in the potential energy surface is found upon adsorption of O-carrying intermediates, that is, a strong O-surface bond is formed. This implies that the TMC(111) surfaces are easily oxidized. Experimental studies show that the O_2 adsorption on TiC(111) [44] and α-Mo_2C(100) [35] are dissociative. Therefore we investigate how the steam reforming reaction is influenced when the TMC(111) and the α-Mo_2C(100) surfaces are oxygenated.

4.2 O-Covered TMC(111) and O-Covered α-Mo_2C(100) Surfaces

Figure 3 shows the calculated potential energy diagram for the steam reforming reaction on the 1ML O-covered TM- and C-terminated TMC surfaces. We find that three of the molybdenum carbide systems the O-covered Mo-terminated δ-MoC(111), the O-covered C-terminated α-Mo_2C(100) and the O-covered Mo-terminated α-Mo_2C(100) surfaces resemble the potential energy of Ni of which the Ni(211) surface is the most active one [2]. The other O-covered surfaces are not suitable as catalysts for the steam reforming either because several of the reaction steps are significantly uphill energetically, or because the surface gets poisoned by some of the intermediates.

We find that, each of the O-covered TMC surfaces is less reactive than its corresponding non-oxidized surface. For a given O-covered TMC surface the TM-terminated surface has higher reactivity than the C-terminated one, in contrast to the finding on the non-oxidized surfaces. For the O-covered TM-terminated TMC surfaces, the reactivity can be ordered as follows α-Mo_2C(100) > δ-MoC(111) > VC(111) > TiC(111), while for the O-covered C-terminated TMC surfaces we find that α-Mo_2C(100) > TiC(111) > VC(111) > δ-MoC(111). The order in reactivity between the different surfaces is thus different for the TM- and for the C-terminated O-covered surfaces.

4.3 TMC(100) Surfaces

The calculated potential energy diagram for the steam reforming reaction on the TMC(100) surfaces is shown in Fig. 4. The δ-MoC(100) surface is found to have a potential energy curve similar to the Ni surfaces. We find a similar shape of the potential energy curves for all the TMC(100) surfaces. A local minimum is found for all the TMC(100) surfaces upon adsorption of CO. The reactivity of the surfaces follows the order δ-MoC(100) > TiC(100) > VC(100), that is, a non linear variation when moving from right to left in the periodic table. Compared to the TMC(111) surface the TMC(100) surfaces are far less reactive. In Ref. [29] it was suggested that the TiC(100) surface is a suitable catalyst for the water–gas-shift reaction. However, according to our calculation it is not the surface of choice for the steam reforming reaction since it is inert (see Fig. 4).

5 Discussion

The conducted computational screening study clearly shows that only molybdenum based carbide surfaces are suitable for the steam reforming reaction. It was found that the δ-MoC(100), the O-covered α-Mo_2C(100) and the O-covered Mo-terminated δ-MoC(111) surfaces have potential energy profiles similar to the one of Ni. The obtained potential energy diagrams show that there is a large variety in the reactivities of the different carbides (see Figs. 2, 3, 4). However, besides the molybdenum carbide

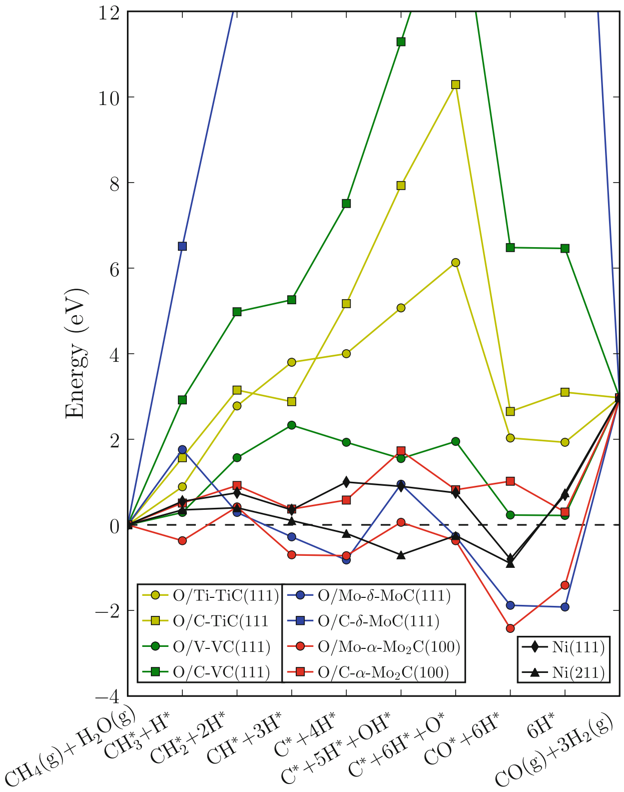

Fig. 3 Calculated potential energy diagram for the 1ML O-covered TM-terminated (*circles*) and C-terminated (*squares*) TMC(111) and α-Mo_2C(100) surfaces. Also given are the Ni(111) and Ni(211) data, adapted from Ref. [2]

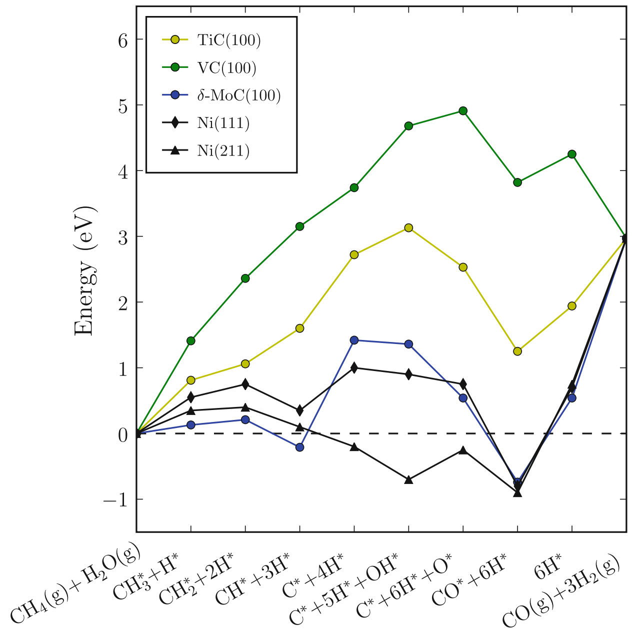

Fig. 4 Calculated potential energy diagram for TMC(100). The Ni(111) and Ni(211) data given here are adapted from Ref. [2]

based surfaces none of the other considered TMC surfaces are suitable for the steam reforming reaction since they either get self-poisoned by the intermediates or they show a significant energetical uphill for some of the elementary steps in Eqs. (2)–(10). Figure 5 shows the preferred adsorptions sites of the considered intermediates on molybdenum based surfaces.

An understanding of the reactivity can be achieved by studying the electronic structure of the surface. In Refs. [15–20] a thorough analysis of the electronic structure established that the TM-terminated TMC(111) surfaces possess surface resonances (SR's). These were identified to be responsible for strong adsorbate-surface bonds. Therefore the high reactivities of the TM-terminated TMC(111) surfaces (see Fig. 2) are attributed to the presence of these SR's. Preliminary electronic structure calculations show that similar resonances are present also on the layered polar α-Mo_2C(100) surfaces, which would explain their high reactivities.

The NaCl TMC(100) surfaces, on the other hand, do not posses any SR's [17, 45] and show a much lower reactivity (see Fig. 4) compared to the TMC(111) surfaces. Since a suitable candidate, the δ-MoC(100) surface, is found among these surfaces we have tried to change the reactivity of the TMC(111) surfaces by weakening their SR's.

The lower reactivities of the O-covered TMC(111) and α-Mo_2C(100) surfaces (see Fig. 3), compared to the corresponding clean surfaces can be understood as follows. Adsorption of oxygen on the TMC(111) results in a quenching of the SR's. Thus, the surfaces are passivated, that is, their ability to form strong bonds with other adsorbates decreases due to the strong O-surface bond. This result shows that the reactivity of carbides surfaces can be tuned.

When it comes to the C-terminated surfaces they also posses SR's in the vicinity of the Fermi level. Intuitively, these SR's should be less pronounced as the C-terminated surfaces can be viewed as a C-covered TM-terminated surface. Hence, the presence of SR's alone can not explain the higher reactivity of the C-terminated surfaces. There is, however, another effect that is present on the C-terminated surfaces namely the interaction between the surface carbon and some of the adsorbates. This gives rise to surface reconstruction and formation of weakly bound intermediates.

An important question for catalytic applications is the stability of the candidate materials. Steam reforming operates over a large range of working conditions with temperatures 700–1,100 °C and pressures 1–25 bar. The most recent phase diagram for Mo–C systems is the one by Velikanova et al. [31] It shows that the bulk α-Mo_2C phase exists for temperatures <1,440 °C, while the δ-MoC is a high temperature phase which exists above 1,956 °C. Based only on bulk data, α-Mo_2C is preferred over δ-MoC.

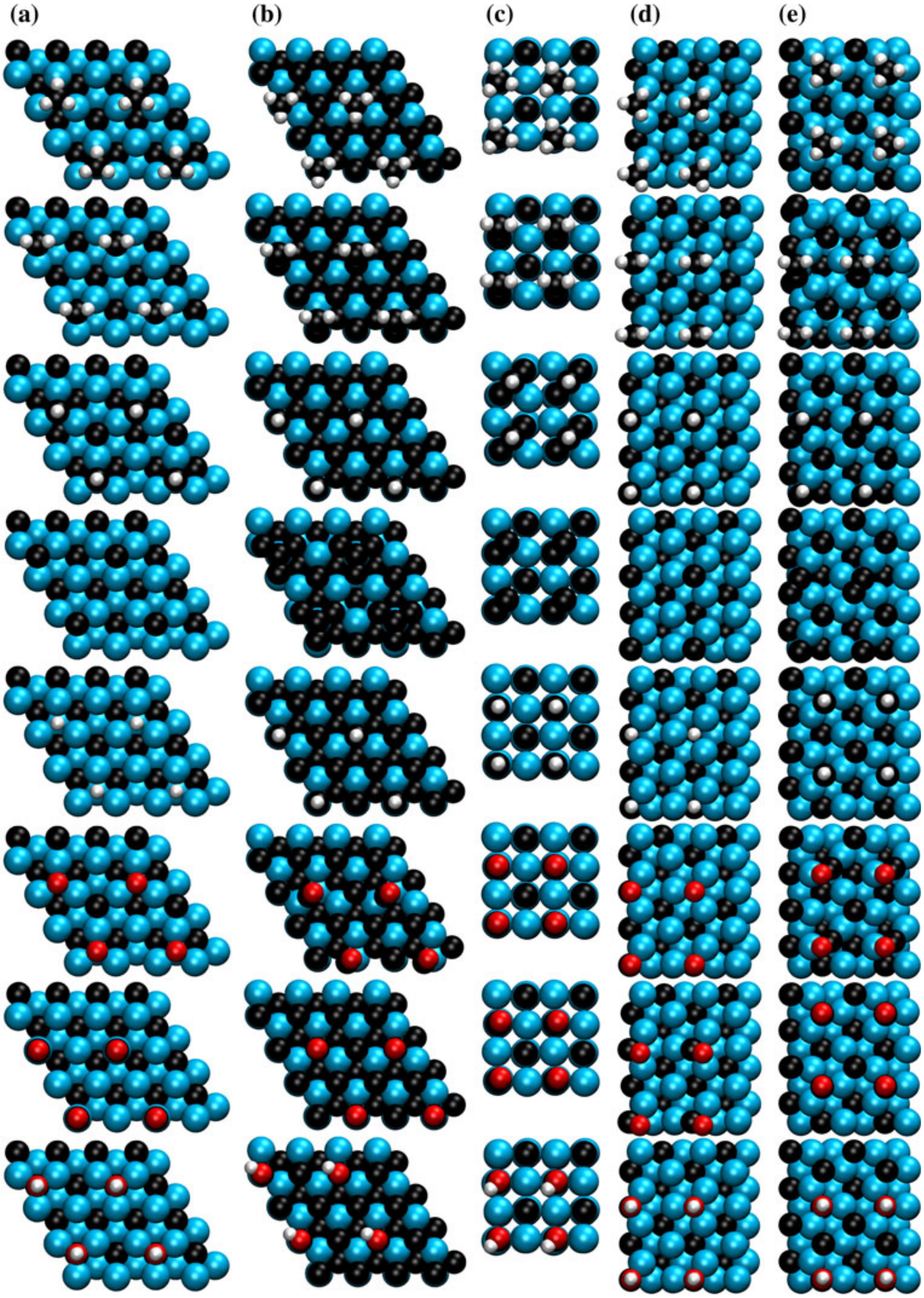

Fig. 5 Top view of the relaxed preferential binding geometries for, from above, CH_3, CH_2, CH, C, H, O, CO and OH for **a** Mo-terminated δ-MoC(111), **b** C-terminated δ-MoC(111), **c** δ-MoC(100), **d** Mo-terminated α-Mo_2C(100), and **e** C-terminated α-Mo_2C(100) surfaces. The *blue*, *black*, *red*, and *white balls* represent Mo, C, O, and H atoms, respectively

When it comes to the stability of a surface the situation can of course differ from the bulk. According to York and coworkers [10, 11], Mo_2C was active and selective for the stoichiometric steam reforming of methane to synthesis gas. The catalyst deactivated at atmospheric pressure, but was very stable when elevated pressures were employed, and no carbon deposition was observed on the catalysts. In those studies the surface characteristics was, however, not addressed.

A surface characterization of α-Mo_2C(100) has been performed in Ref. [34]. The surface preparation consisted of Ar ion bombardment followed by annealing at successively higher temperatures. The surface was found to change from being Mo terminated to C terminated at annealing temperatures above 1,300 K. Despite that these surfaces are stable at temperatures relevant for the steam reforming, our study shows that they are too reactive. Adsorption of O_2 on both the Mo- and the C-terminated α-$Mo_2C(100)$ surfaces were found to be dissociative and the surfaces were covered with oxygen at 800 K [35]. This supports the stability of the O-covered α-$Mo_2C(100)$ surfaces.

In addition, stable crystalline molybdenum carbide films prepared by chemical vapor deposition (CVD) and physical vapor deposition (PVD) have been found to contain either Mo_2C and/or the δ-MoC_{1-x} phase [46–49]. Hence it seems plausible that both the O-covered α-$Mo_2C(100)$ and the δ-MoC(100) surfaces may be stable at relevant steam reforming conditions. However, further studies are needed to address the formation of oxycarbide and what the stable carbon and oxygen coverages are under different reaction conditions.

6 Conclusion

In this paper, a computational screening study of the steam reforming reaction on transition-mental carbides has been presented. By using a screening approach we are able to map out the large reactivity space, which ranges from very reactive to inert, provided by the carbides. This study clearly shows, solely based on thermochemical data, that a steam reforming carbide catalyst should be molybdenum based and most probably have oxygen on the surface in some form. Also, this study illustrates the versatility and tunability of the TMC systems. The results can be understood in terms of the previously proposed model of chemisorption on TMC surfaces, in which surface resonances play crucial roles. Future studies should address surface stability in the presence of carbon and oxygen under various conditions, as well as coverage and coadsorption effects. In addition, more detailed studies of surface electronic structure and kinetics are needed to establish what surface characteristics that are required of a carbide to make it a suitable catalyst for steam reforming.

Acknowledgments The author acknowledges support from the Swedish Research Council and from the U.S. Department of Energy, Office of Basic Energy Sciences. The calculations were performed at HPC2N via the Swedish National Infrastructure for Computing. The author thanks Anders Hellman, Carlo Ruberto, Bengt I. Lundqvist and Jens K. Nørskov for constructive discussions and comments on the manuscripts.

References

1. Rostrup-Nielsen JR, Sehested J, Nørskov JK (2002) Adv Catal 47:65
2. Bengaard HS, Nørskov JK, Sehested J, Clausen BS, Nielsen LP, Molenbroek AM, Rostrup-Nielsen JR (2002) J Catal 209:365
3. Helveg S, López-Cartes C, Sehested J, Hansen PL, Clausen BS, Rostrup-Nielsen JR, Abild-Pedersen F, Nørskov JK (2004) Nature 427:426
4. Jones G, Jakobsen JG, Shimb SS, Kleis J, Andersson MP, Rossmeisl J, Abild-Pedersen F, Bligaard T, Helveg S, Hinnemann B, Rostrup-Nielsen JR, Chorkendorff I, Sehested J, Nørskov JK (2008) J Catal 259:147
5. Levy RB, Boudart M (1973) Science 181:547
6. Volpe L, Boudart M (1985) J Solid State Chem 59:348
7. Lee JS, Oyama ST, Boudart M (1987) J Catal 106:125
8. Lee JS, Lee KH, Lee JY (1992) J Phys Chem 96:362
9. Oyama ST (1996) In: Oyama ST (ed) The chemistry of transition metal carbides and nitrides. Blackie Academic and Professional, Glasgow
10. York APE, Claridge JB, Brungs AJ, Tsang SC, Green MLH (1997) Chem Commun 1:39
11. Claridge JB, York APE, Brungs AJ, Marquez-Alvares C, Sloan J, Tsang SC, Green MLH (1998) J Catal 180:85
12. Zhang YF, Li JQ, Zhou LX (2001) Surf Sci 488:256
13. Kitchin J, Nørskow JK, Barteau MA, Chen JG (2005) Catal Today 105:66
14. Viñes F, Sousa C, Illas F, Liu P, Rodriguez JA (2007) J Phys Chem C 111:1307
15. Vojvodic A, Ruberto C, Lundqvist BI (2006) Surf Sci 600:3619
16. Ruberto C, Vojvodic A, Lundqvist BI (2006) Surf Sci 600:1612
17. Ruberto C, Lundqvist BI (2007) Phys Rev B 75:235438
18. Ruberto C, Vojvodic A, Lundqvist BI (2007) Solid State Commun 141:48
19. Vojvodic A, Ruberto C, Lundqvist BI (2010) J Phys Condens Matter 22:375504
20. Vojvodic A, Hellman A, Ruberto C, Lundqvist BI (2009) Phys Rev Lett 103:146103
21. Viñes F, Sousa C, Illas F, Liu P, Rodriguez JA (2007) J Phys Chem C 111:16982
22. Didziulis SV, Frantz P, Fernandez-Torres LC, Guenard RL, El-bjeirami O, Perry SS (2001) J Phys Chem 105:5196
23. Liu P, Rodriguez JA (2004) J Chem Phys 120:5414
24. Ren J, Huo C-F, Wang J, Jiao H (2005) Surf Sci 596:212
25. Pistonesi C, Juan A, Farkas AP, Solymosi F (2008) Surf Sci 602:13
26. Ren J, Huo C-F, Wang J, Cao Z, Li Y-W, Jiao H (2006) Surf Sci 600:2329
27. Tominaga H, Hagai M (2005) J Phys Chem B 109:20415
28. Liu P, Rodriguez JA (2006) J Phys Chem B 110:19418
29. Viñes F, Rodriguez JA, Liu P, Illas F (2008) J Catal 260:103
30. Dubois J, Epicier T, Esnouf C, Fantozzi G, Convert P (1988) Acta Metall 36:1891
31. Velikanova TY, Kublii VZ, Khaenko BV (1988) Soviet Powder Metall Met Ceram 27:891
32. Parthe E, Sadagopan V (1963) Acta Crystallogr 16:202
33. Otani S, Ishizawa Y (1995) J Cryst Growth 154:202
34. St. Clair TP, Oyama ST, Cox DF, Otani S, Ishizawa Y, Lo R-L, Fukui K, Iwasawa Y (1999) Surf Sci 426:187
35. St. Clair TP, Oyama ST, Cox DF (2000) Surf Sci 468:62
36. Bahn SR, Jacobsen KW (2002) Comput Sci Eng 4:56. http://wiki.fysik.dtu.dk/dacapo
37. Hammer B, Hansen LB, Nørskov JK (1999) Phys Rev B 59:7413
38. Fu C-L, Ho K-M (1983) Phys Rev B 28:5480
39. Nakamura K, Yashima M (2005) Mater Sci Eng B 148:69
40. Férnandez Guillermet A, Häglund J, Grimvall G (1992) Phys Rev B 45:11557
41. Nørskov JK, Bligaard T, Logadottir A, Bahn S, Hansen LB, Bollinger M, Bengaard H, Hammer B, Sljivancanin Z, Mavrikakis M, Xu Y, Dahl S, Jacobsen CJH (2002) J Catal 209:275
42. Aono M, Oshima C, Zaima S, Otani S, Ishizawa Y (1981) Jpn J Appl Phys 20:L829
43. Rundgren J, Gauthier Y, Baudoing-Savois R, Joly Y, Johansson LI (1992) Phys Rev B 45:4445

44. Brandshaw AM, van der Veen JF, Himpsel FJ, Eastman DE (1980) Solid State Commun 37:37
45. Oshima C, Aono M, Zaima S, Shibata Y, Kawai S (1981) J Less-Common Met 82:69
46. Wood J, Chen JE, Kadin AM, Burkhardt RW, Ovshinsky SR (1985) IEEE Trans Magn 21:842
47. Haase EL (1987) J Low Temp Phys 69:245
48. Okuyama F, Fujimoto Y, Kato S, Kondo H (1985) Appl Phys A 38:275
49. Lu J, Hugosson H, Eriksson O, Nordström L, Jansson U (2000) Thin Solid Films 370:203